Reimei Workshop "Hadrons in dense matter at J-PARC", February 21 - 23, 2022
in hybrid style（on-site (KEK Tokai Campus, Ibaraki, Japan) and online）

Recent topics on $\pi^-, K^-, \eta(958)$ mesonic bound states

Satoru Hirenzaki (Nara Women's University, Japan)

16.00 - 16.30, Feb. 23 (Wednesday)

【0】Introduction

<u>schematic view of the mass of π, K, η & η'</u>

(3) Aspects of the Strong Int. Symmetry

Jido *et al.*, PRC85(12)032201(R)
Nagahiro *et al.*, PRC (2013)

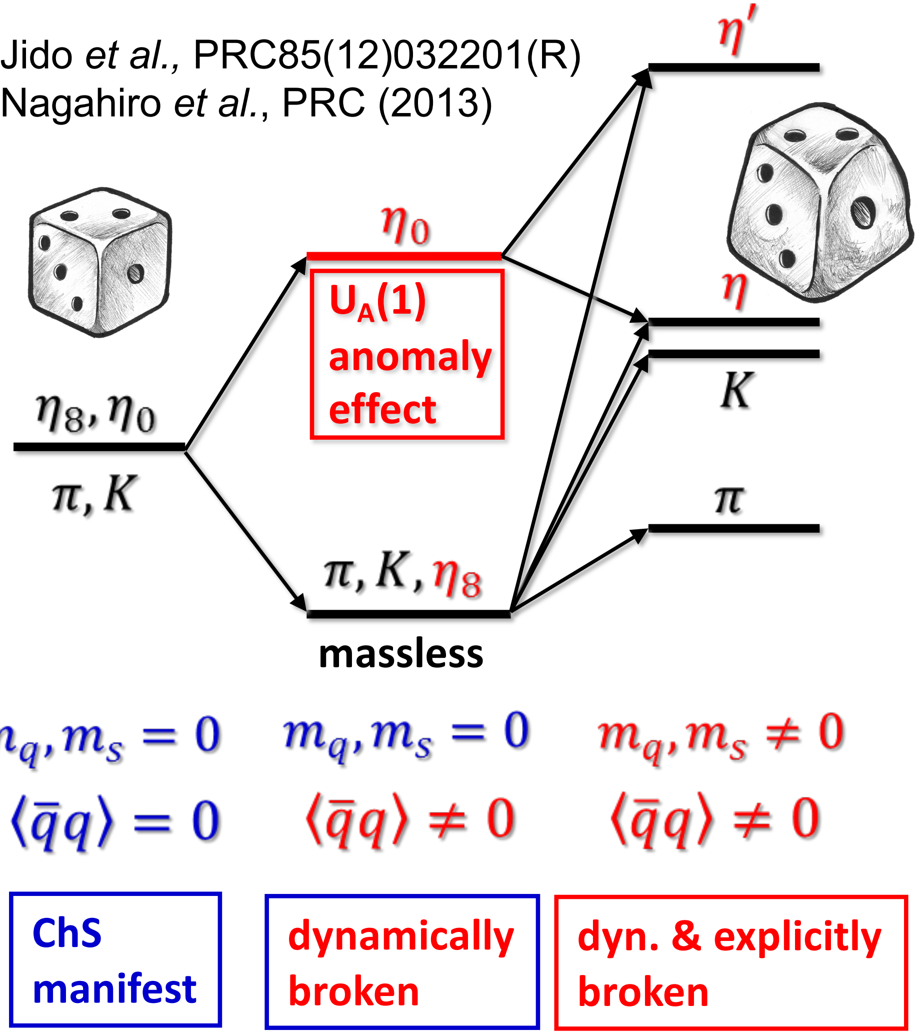

【0】Introduction

【1】Pionic Atom and $\sigma_{\pi N}$
with high-precision data at RIBF/RIKEN

【2】Kaonic atom in ^{3,4}He

【3】 $\eta(958)$ state in (p, dp)

【4】Summary

Deeply Bound Pionic Atom by (d,³He) @ GSI

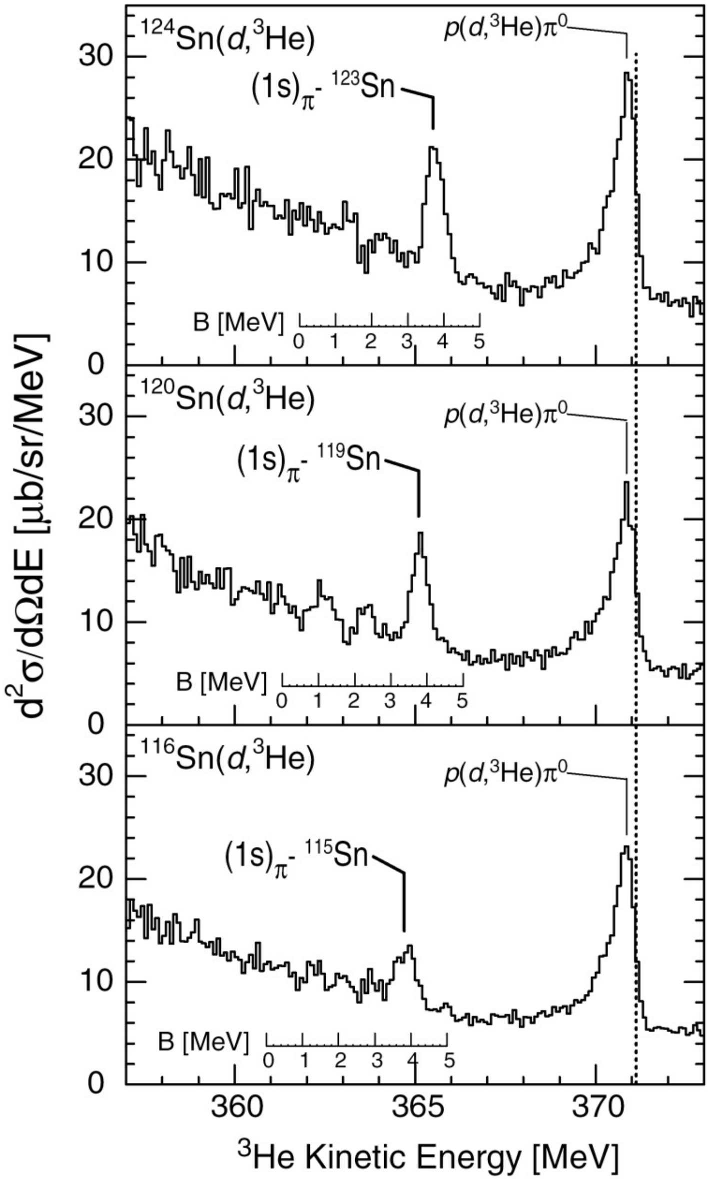

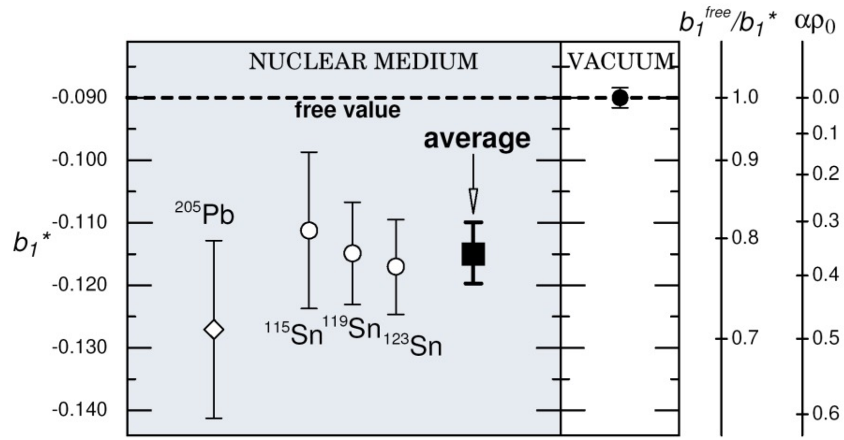

K. Suzuki *et al.*

Phys. Rev. Lett. 92(2004) 072302

GOR relation + Tomozawa-Weinberg Relation

$$\frac{\langle \bar{q}q \rangle_\rho}{\langle \bar{q}q \rangle_0} \simeq \frac{f_\pi^{*2}}{f_\pi{}^2} \simeq \frac{b_1^{\mathrm{free}}}{b_1^*(\rho)} = 0.78 \pm 0.05 \ @ \ \rho \simeq 0.6\rho_0$$

$$\sim 0.64 \ @ \ \rho = \rho_0$$

Sensitivity of the deeply bound pionic atom observables to the pion-nucleon sigma term $\sigma_{\pi N}$

By Natumi Ikeno (Tottori univ.), S. H.

$$\left[-\nabla^2 + \mu^2 + 2\mu V_{\rm opt}(r)\right] \phi(\vec{r}) = \left[E - V_{\rm em}(r)\right]^2 \phi(\vec{r}),$$

$$2\mu V_{\rm opt}(r) = -4\pi[b(r) + \varepsilon_2 B_0 \rho^2(r)] + 4\pi\nabla\cdot[c(r) + \varepsilon_2^{-1} C_0 \rho^2(r)]L(r)\nabla,$$

$$\begin{aligned} b(r) &= \varepsilon_1[b_0\rho(r) + b_1[\rho_n(r) - \rho_p(r)]], \\ c(r) &= \varepsilon_1^{-1}[c_0\rho(r) + c_1[\rho_n(r) - \rho_p(r)]], \\ L(r) &= \left\{1 + \frac{4}{3}\pi\lambda[c(r) + \varepsilon_2^{-1} C_0 \rho^2(r)]\right\}^{-1}, \end{aligned}$$

$$b_1(\rho) = b_1^{\rm free}\left(1 - \frac{\sigma_{\pi N}}{m_\pi^2 f_\pi^2}\rho\right)^{-1}, \qquad b_0(\rho) = b_0^{\rm free} - \varepsilon_1 \frac{3}{2\pi}(b_0^{\rm free2} + 2b_1^2(\rho))\left(\frac{3\pi^2}{2}\rho\right)^{1/3}$$

Tomozawa-Weinberg, GOR.

K. Suzuki *et al.*
Phys. Rev. Lett. 92(2004) 072302

$$\frac{\langle\bar{q}q\rangle_\rho}{\langle\bar{q}q\rangle_0} \simeq \frac{f_\pi^{*2}}{f_\pi^{2}} \simeq \frac{b_1^{\rm free}}{b_1^*(\rho)} = 0.78 \pm 0.05 \ @ \ \rho \simeq 0.6\rho_0$$ ➔ σ ~ 45MeV

χ^2 fitting for atomic data (BE, Width) $\quad \sigma_{\pi N}^{\rm FG} = 57 \pm 7$ MeV,

E. Friedman and A. Gal, Phys. Lett. B **792**, 340 (2019).
E. Friedman and A. Gal, Acta Phys. Polon. B **51**, 45-54 (2020).

$\sigma_{\pi N}$ values

$$\sigma_{\pi N} = \frac{\bar{m}_q}{2m_N} \sum_{u,d} \langle N|\bar{q}q|N\rangle \qquad \bar{m}_q = \frac{m_u + m_d}{2}$$

Nucleon charges with dynamical overlap fermions

PHYSICAL REVIEW D **98,** 054516 (2018)

N. Yamanaka* et al., (JLQCD Collaboration)

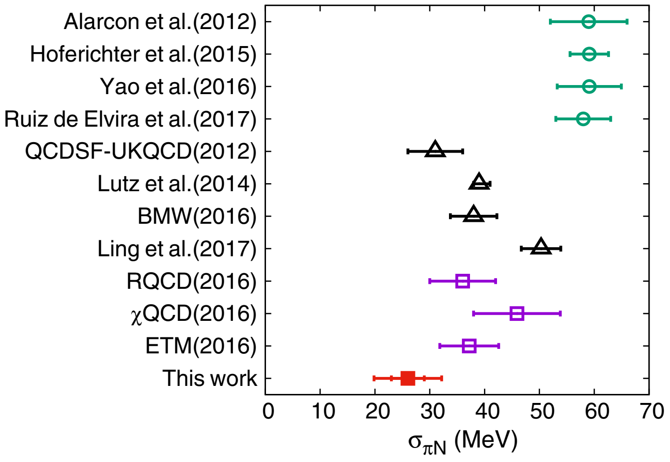

FIG. 13. Our result for $\sigma_{\pi N}$ (filled square) compared with those from recent direct evaluations in lattice QCD (open squares, RQCD [9], χQCD [8], ETM [11]), analyses of lattice QCD data using Feynman-Hellmann theorem (black triangles, QCDSF-UKQCD [7], Lutz *et al.* [74], BMW [10], Ling *et al.* [75]) and phenomenological studies (open circles, Alarcón *et al.* [12], Hoferichter *et al.* [13], Yao *et al.* [15], Ruiz de Elvira *et al.* [16]). As for our result, the smallest error bar denotes the statistical one, and the largest one also takes into account those due to the extrapolation and the discretization.

The nucleon sigma term from lattice QCD

R. Gupta, S. Park, M. Hoferichter, E. Mereghetti, B. Yoon and T. Bhattacharya, Phys. Rev. Lett. **127**, 24 (2021).

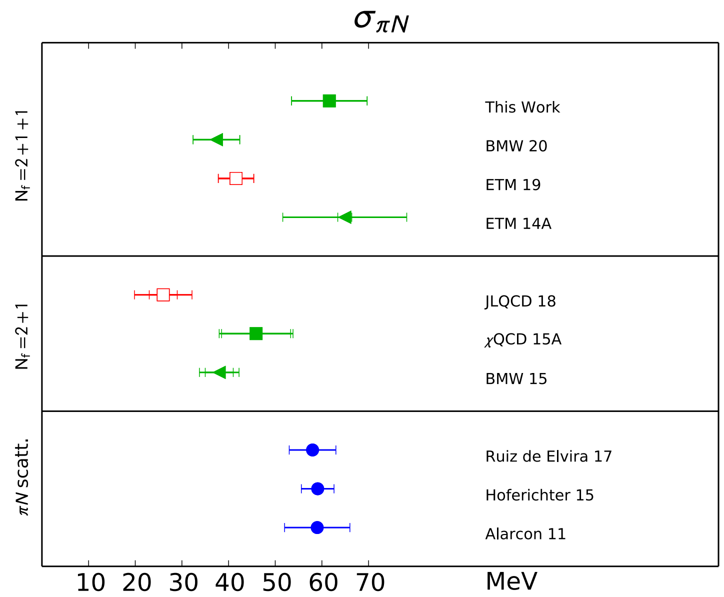

FIG. 8. Results for $\sigma_{\pi N} = m_{ud} g_S^{u+d}$ from 2+1- and 2+1+1-flavor lattice calculations. The BMW 20 result from 1+1+1+1-flavor lattices is listed along with the other 2+1+1-flavor calculations for brevity. Following the FLAG conventions, determinations via the direct approach are indicated by squares and the FH method by triangles. Also, the symbols used for lattice estimates that satisfy the FLAG criteria for inclusion in averages are filled green, and those not included are open red. The references from which lattice results have been taken are: JLQCD 18 [60], χQCD 15A [57], BMW 15 [56], ETM 14A [63], ETM 19 [61], and BMW 20 [62]. Phenomenological estimates using πN scattering data (blue filled circles) are from Alarcon 11 [28], Hoferichter 15 [31], and Ruiz de Elvira 17 [37].

Cf. $\sigma_{\pi N}^{\mathrm{FG}} = 57 \pm 7$ MeV,

Latest Data @ RIKEN

Spectroscopy of Pionic Atoms in ^{122}Sn$(d,{}^3$He$)$ Reaction and Angular Dependence of the Formation Cross Sections

PHYSICAL REVIEW LETTERS **120,** 152505 (2018)

T. Nishi, K. Itahashi et al., (piAF Collaboration)

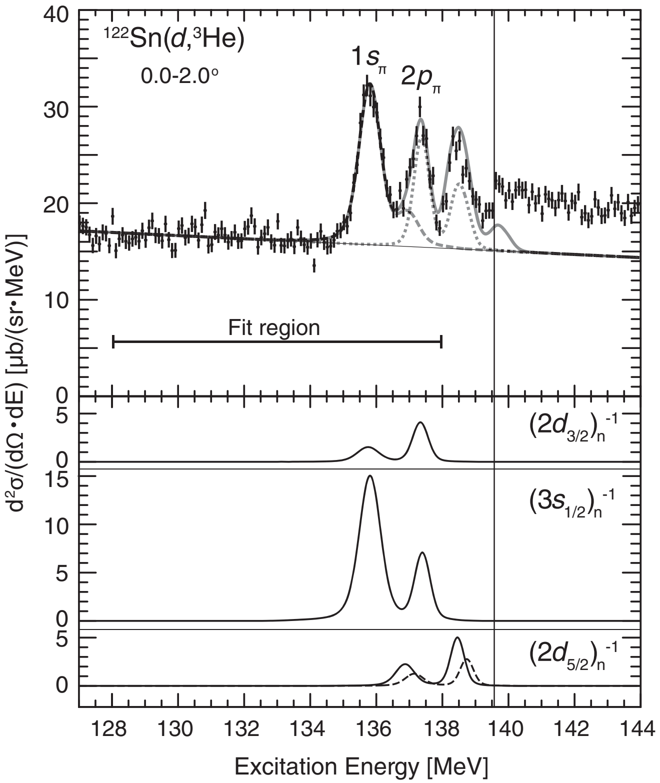

FIG. 2. (Top panel) Measured excitation spectrum of the ^{122}Sn$(d, {}^3$He$)$ reaction at the angular range of $0 < \theta < 2°$. Three distinct peaks are observed in the region $E_{ex} = [134, 139]$ MeV. The left and middle peaks are mainly originating from formation of pionic $1s$ and $2p$ states, respectively. The right peak is partly contributed from the other pionic states ($2s$, $3p$, and $3s$). The spectrum is fitted in the region indicated. The fitting curve and contributions from the $1s$ and the $2p$ states are presented by solid, dashed, and dotted lines, respectively. (Bottom panel) Decom-

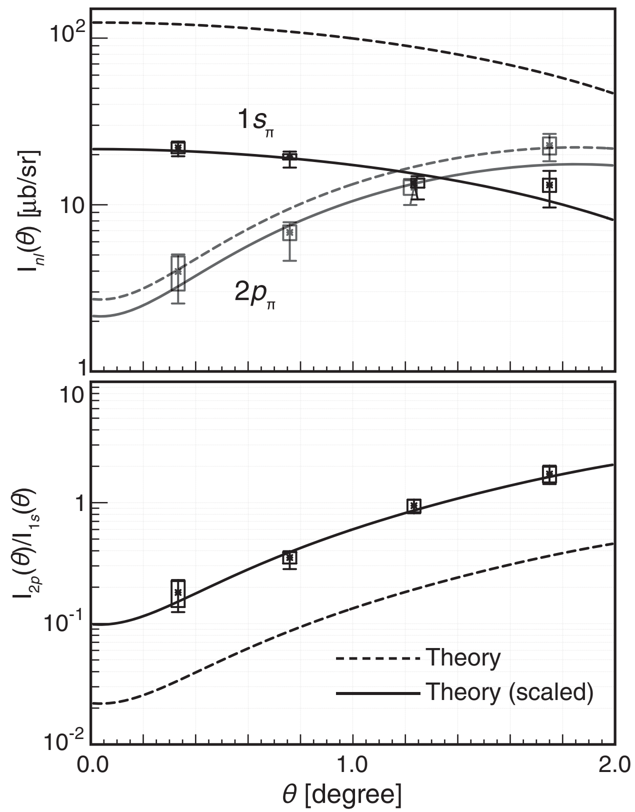

FIG. 4. (Top panel) Determined pionic-nl-state formation cross sections $I_{nl}(\theta)$ for different θ ranges. Statistical errors are shown by the boxes and systematic errors in addition by the bars. The deduced cross sections are compared with the theoretical calculations [19,28]. (Bottom panel) $I_{2p}(\theta)/I_{1s}(\theta)$. Systematic errors are canceled by taking the ratios.

Sensitivity of the deeply bound pionic atom observables to the pion-nucleon sigma term $\sigma_{\pi N}$

By Natumi Ikeno (Tottori univ.)

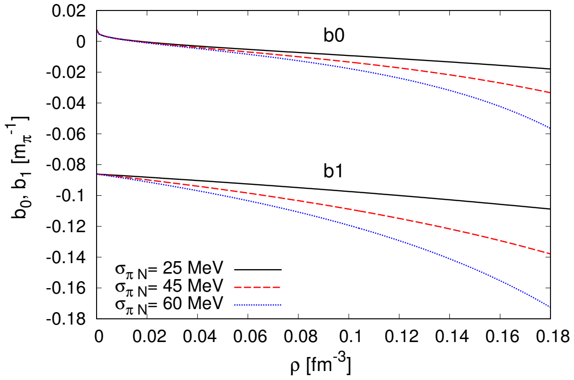

FIG. 1: Density dependence of the $b_0(\rho)$ and $b_1(\rho)$ for the different $\sigma_{\pi N}$ term.

$$b_1(\rho) = b_1^{\rm free}\left(1 - \frac{\sigma_{\pi N}}{m_\pi^2 f_\pi^2}\rho\right)^{-1},$$

$$b_0(\rho) = b_0^{\rm free} - \varepsilon_1 \frac{3}{2\pi}(b_0^{\rm free2} + 2b_1^2(\rho))\left(\frac{3\pi^2}{2}\rho\right)^{1/3}$$

$$\frac{\Delta BE(1s)}{\Delta\sigma_{\pi N}} \sim \frac{6keV}{1MeV}$$

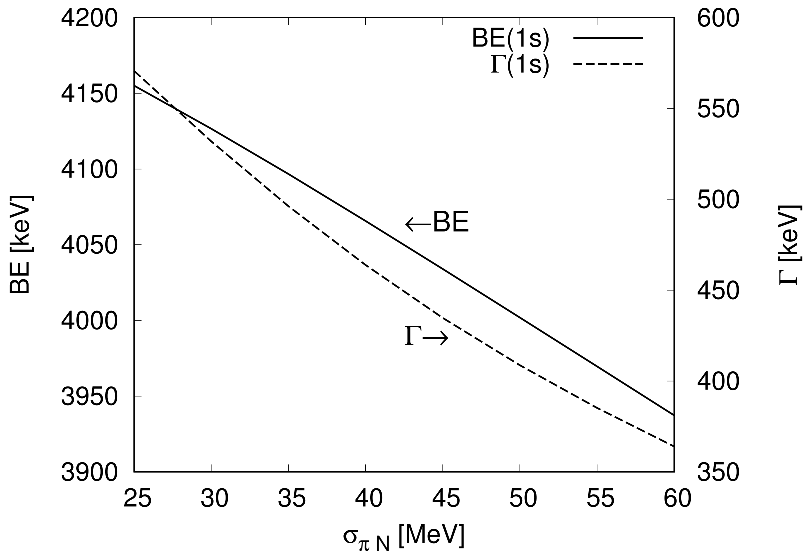

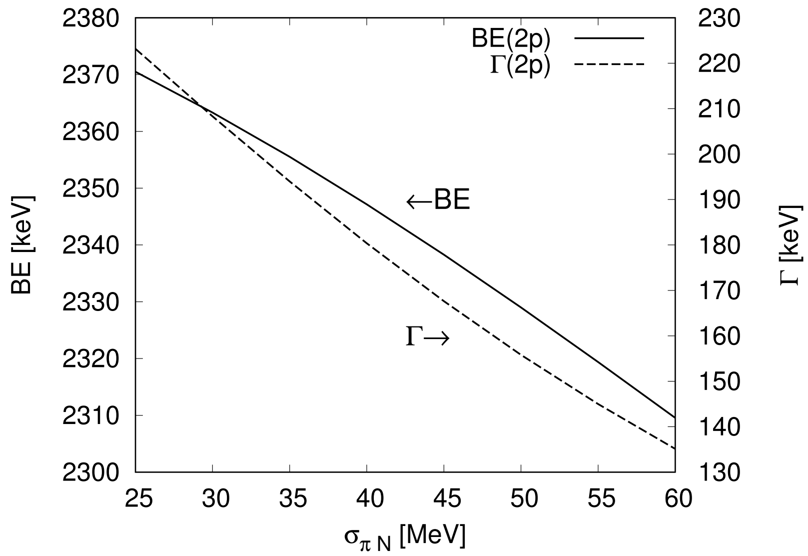

FIG. 2: Binding energies (B.E.) and widths (Γ) of the pionic 1s and 2p states in ^{123}Sn as a function of $\sigma_{\pi N}$. The results correspond to the calculation with the parameter set (I).

Sensitivity of the deeply bound pionic atom observables to the pion-nucleon sigma term $\sigma_{\pi N}$

By Natumi Ikeno (Tottori univ.)

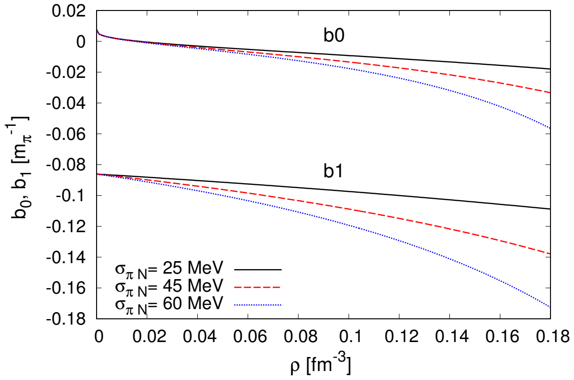

FIG. 1: Density dependence of the $b_0(\rho)$ and $b_1(\rho)$ for the different $\sigma_{\pi N}$ term.

$$b_1(\rho) = b_1^{\text{free}} \left(1 - \frac{\sigma_{\pi N}}{m_\pi^2 f_\pi^2}\rho\right)^{-1},$$

$$b_0(\rho) = b_0^{\text{free}} - \varepsilon_1 \frac{3}{2\pi}(b_0^{\text{free2}} + 2b_1^2(\rho)) \left(\frac{3\pi^2}{2}\rho\right)^{1/3}$$

Extra sensitivities beyond BE and width ?

(d,^{3}He) spectra

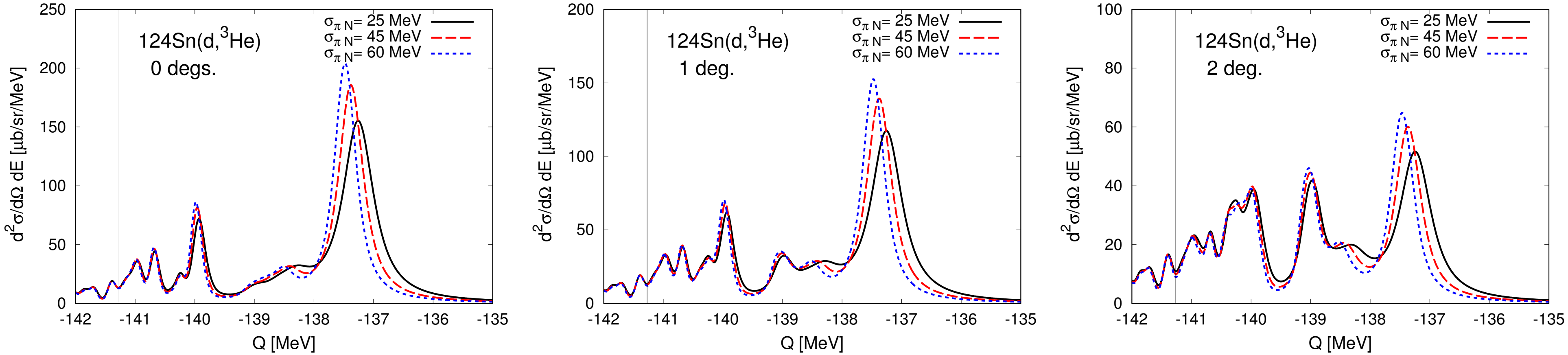

FIG. 4: Formation cross section in the ^{124}Sn$(d,{}^3$He$)$ reaction for the different angles. Left, middle and right panel is the result for $\theta_{\rm dHe} = 0^\circ, 1^\circ, 2^\circ$, respectively. The calculations are done with the parameter set (I). Experimental energy resolution is assumed to be $\Delta E = 150$ keV

Sensitivity of the deeply bound pionic atom observables to the pion-nucleon sigma term $\sigma_{\pi N}$

By Natumi Ikeno (Tottori univ.)

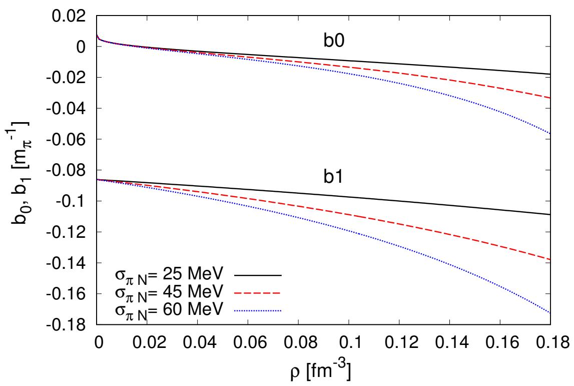

FIG. 1: Density dependence of the $b_0(\rho)$ and $b_1(\rho)$ for the different $\sigma_{\pi N}$ term.

$$b_1(\rho) = b_1^{\mathrm{free}} \left(1 - \frac{\sigma_{\pi N}}{m_\pi^2 f_\pi^2}\rho\right)^{-1},$$

$$b_0(\rho) = b_0^{\mathrm{free}} - \varepsilon_1 \frac{3}{2\pi}(b_0^{\mathrm{free}2} + 2b_1^2(\rho)) \left(\frac{3\pi^2}{2}\rho\right)^{1/3}$$

Dr. Ikeno will summarize the results soon !

(d,^{3}He) angular distribution（INsensitive !）

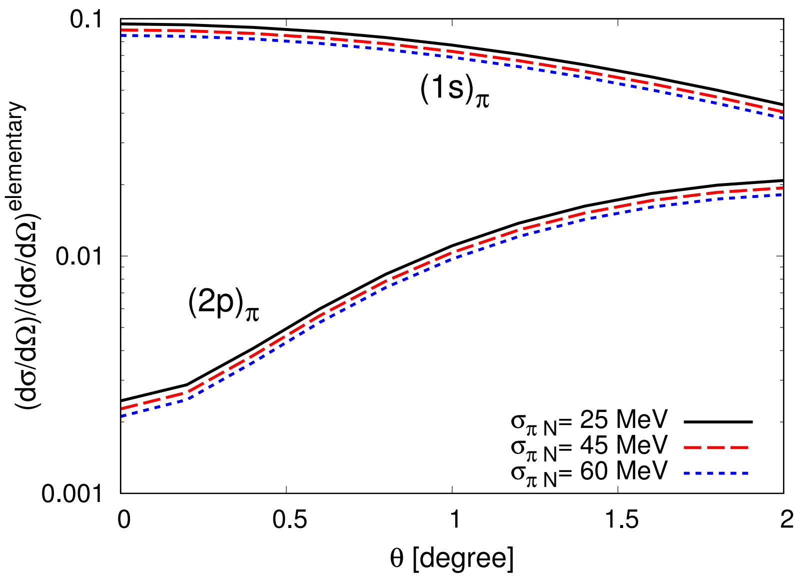

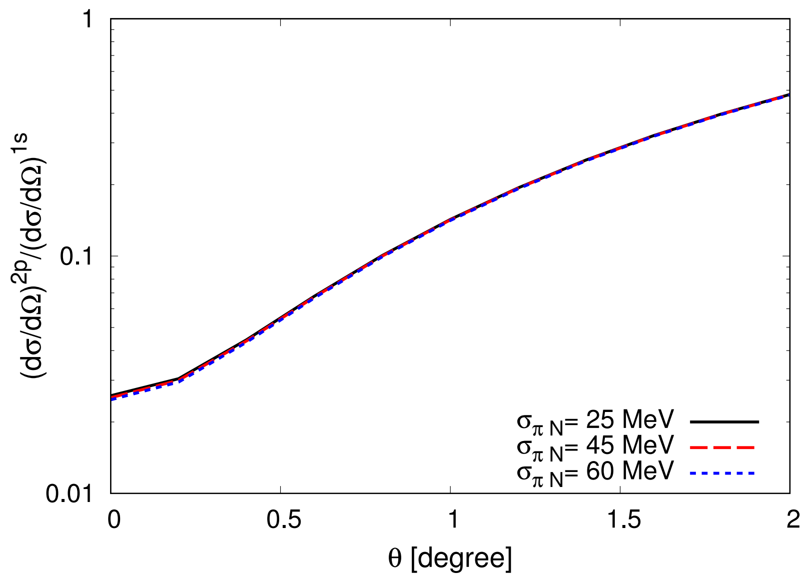

Kaonic atom in ^{3,4}He

Hirenzaki, Okumura, Toki, Oset, Ramos
PRC61(2000)055205

anomalous shift

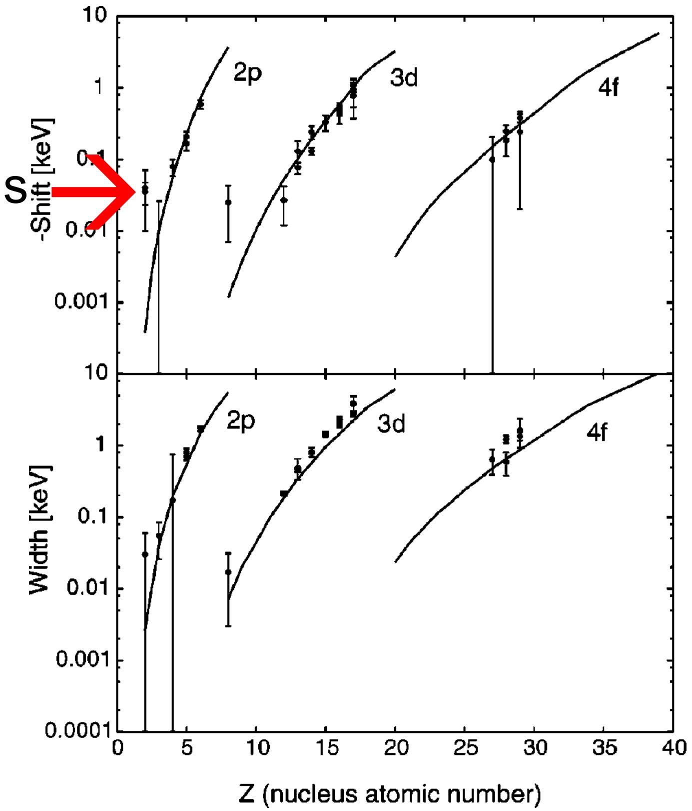

FIG. 3. The calculated energy shifts and widths are shown as functions of the nucleus atomic number for $2p$, $3d$, and $4f$ kaonic atom states. Experimental data are also shown [20].

Mystery in last century

and this century

Y. Akaishi, Proc. of EXA2005 (2006) 45-53

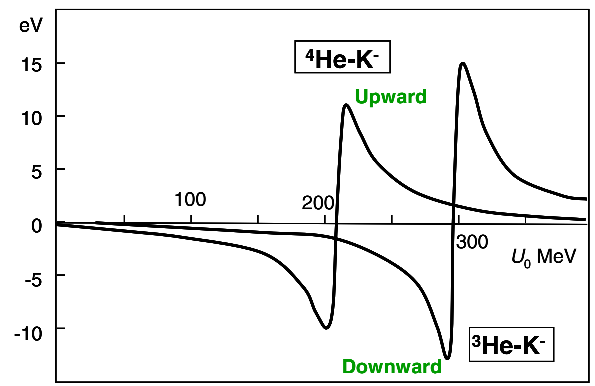

Figure 4: $2p$ level shifts of the K^--^{4}He and K^--^{3}He atoms calculated by the use of the coupled-channel model with $U_{\mathrm{coupl}} = 120$ MeV.

Large shift and width
<—> Generation of new nuclear state

Kaonic atom in $^{3,4}He$

Measurements of Strong-Interaction Effects in Kaonic-Helium Isotopes at Sub-eV Precision with X-Ray Microcalorimeters

T. Hashimoto, (J-PARC E62 Collaboration)

PRL accepted (2022)

X-ray, 3d→2p process, ^3He and ^4He

shift + width error ~ 1eV

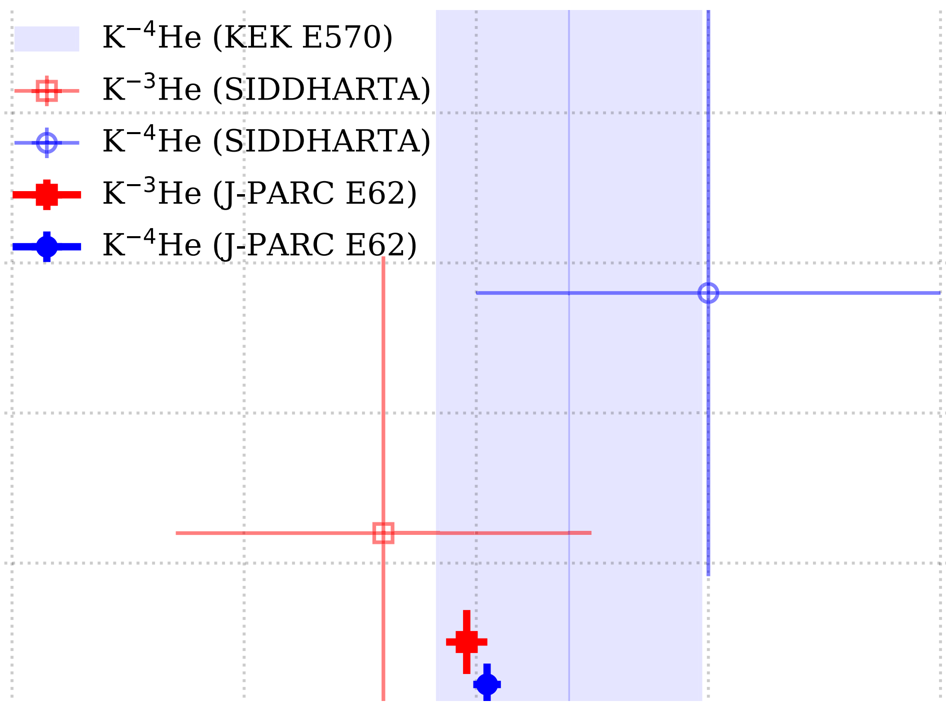

Figure: Just to impress you the <u>smallness of the error</u> !!

Please consult the published paper.

Kaonic atom in 3, 4He

* Comparison with the latest data is in progress.
* Potentials based on Chiral unitary model and Phenomenological (non-linear) potential are also considered.

Dr. Yamagata-Sekihara will obtain the results soon !

$$V(r) = (V_0 + iW_0)\frac{\rho(r)}{\rho_0}$$

$^3\mathrm{He} - K$

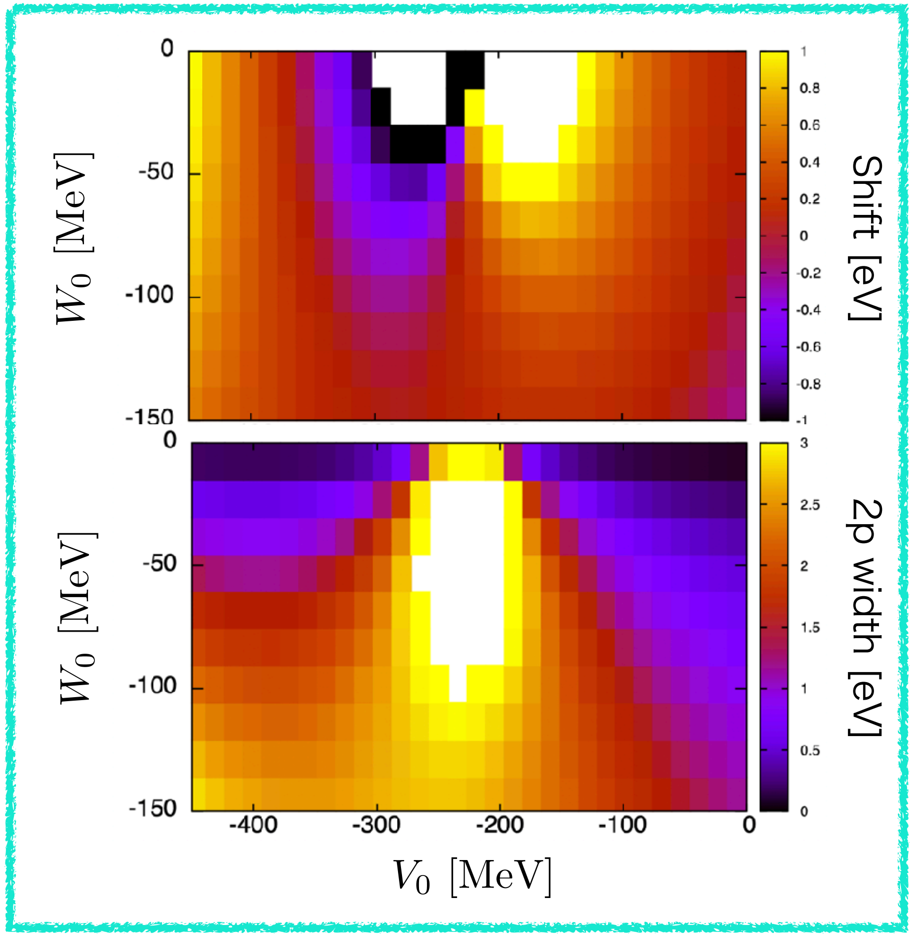

$^4\mathrm{He} - K$

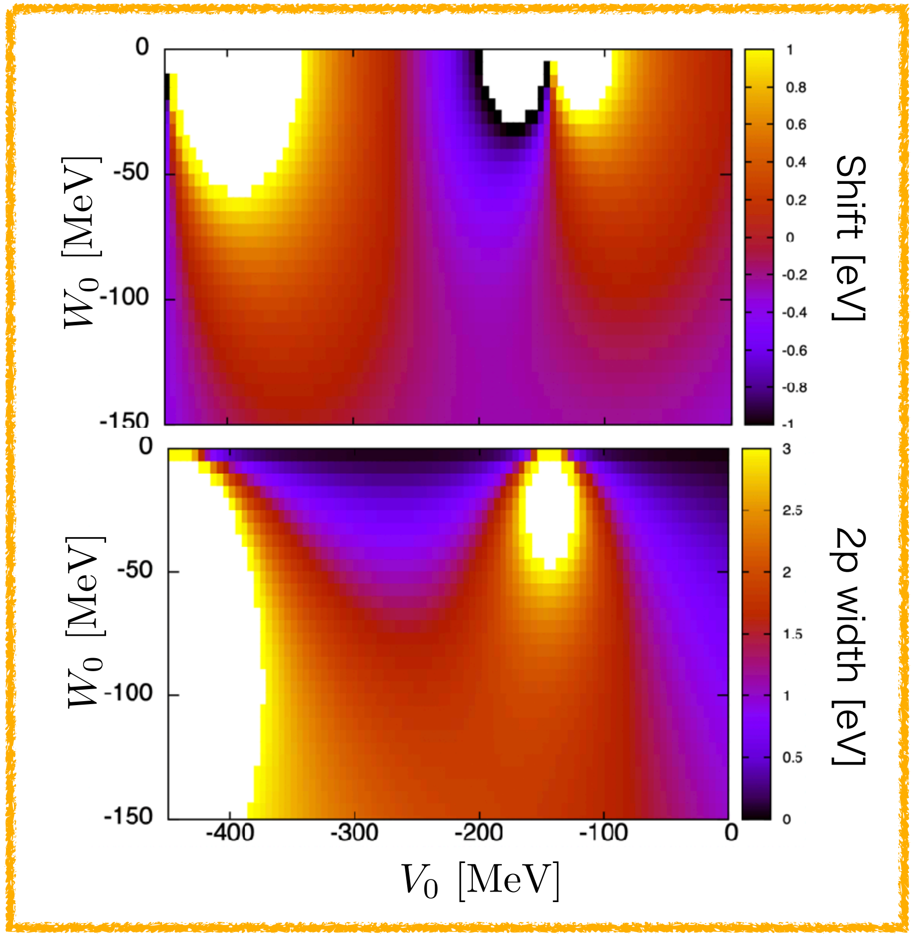

$\eta(958)$ state

<u>schematic view of the mass of π, K, η & η'</u>

Jido *et al.*, PRC85(12)032201(R)
Nagahiro *et al.*, PRC (2013)

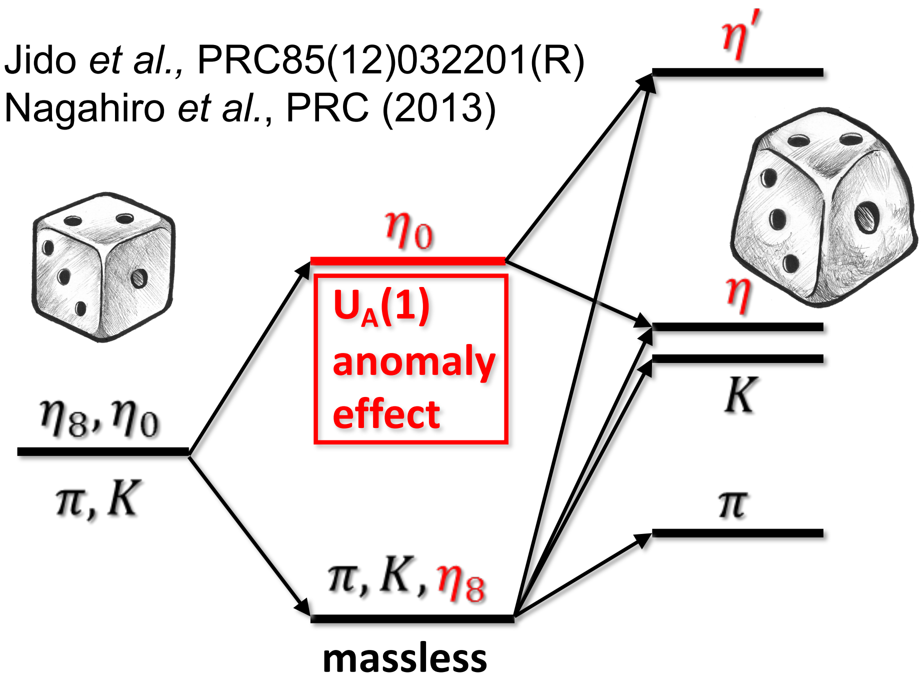

$m_q, m_s = 0$ | $m_q, m_s = 0$ | $m_q, m_s \neq 0$

$\langle \bar{q}q \rangle = 0$ | $\langle \bar{q}q \rangle \neq 0$ | $\langle \bar{q}q \rangle \neq 0$

ChS manifest | **dynamically broken** | **dyn. & explicitly broken**

<u>*ex.)* NJL model with KMT</u>

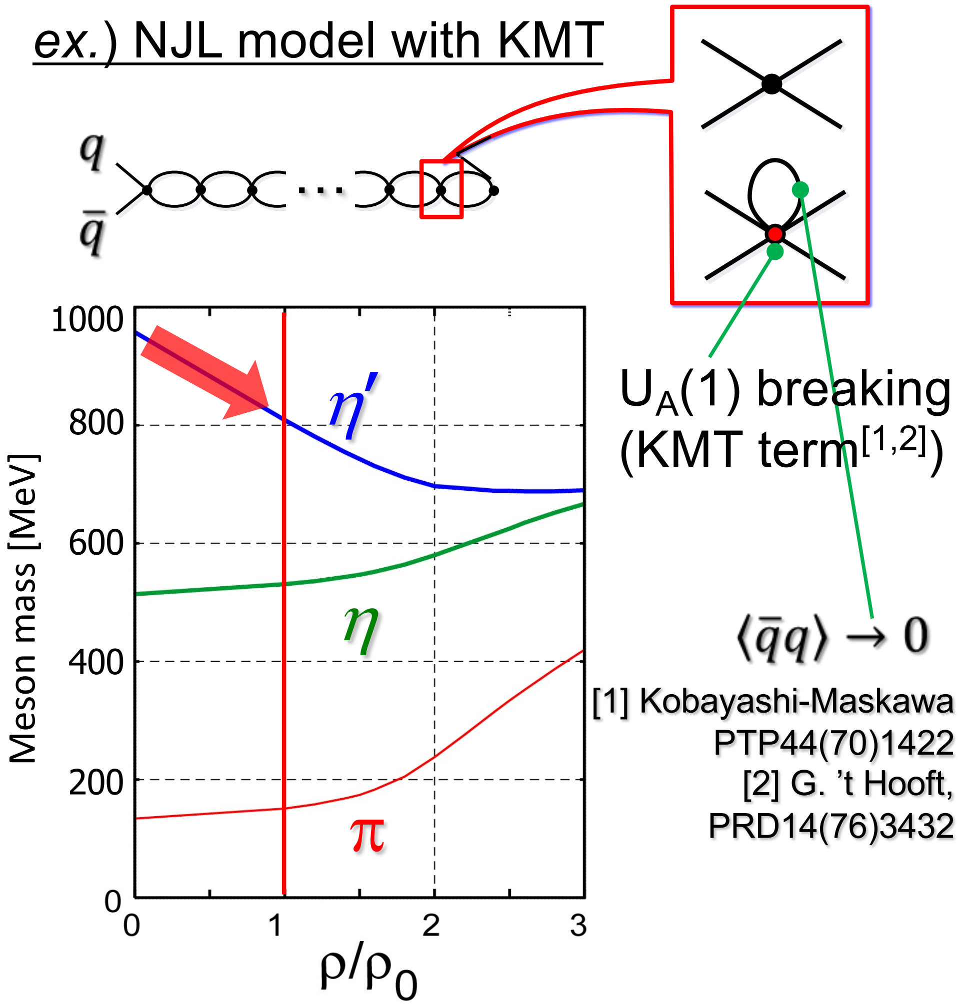

[1] Kobayashi-Maskawa PTP44(70)1422
[2] G. 't Hooft, PRD14(76)3432

$\Delta m \sim -150$ MeV @ ρ_0

Costa *et al.*,PLB560(03)171,
Nagahiro, Takizawa, Hirenzaki, PRC74(06)045203

$\eta(958)$ state

Formation by (p,d) is theoretically predicted.

$$V_{\eta'}(r) = (V_0 + iW_0)\,\frac{\rho(r)}{\rho_0}$$

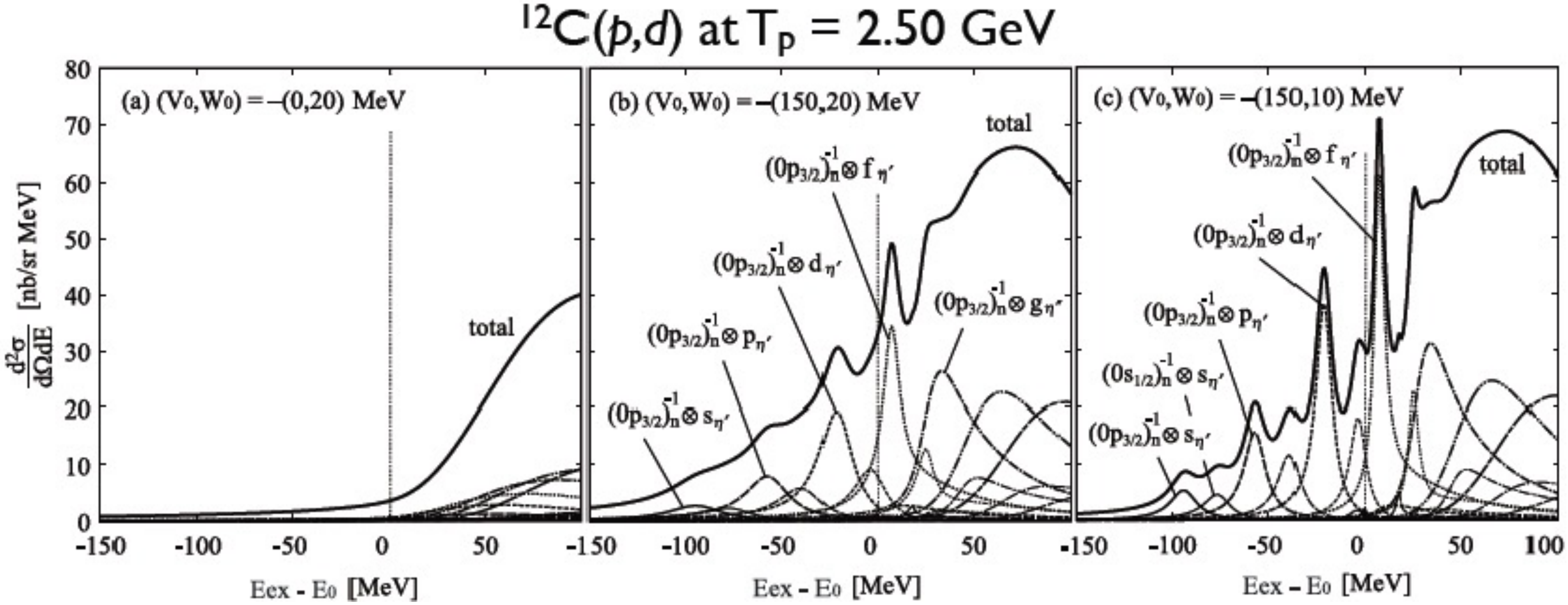

Nagahiro et al., PRC87(13)045201.

(η-PRiME/Super-FRS Collaboration)

Experimental Results
（Huge background）

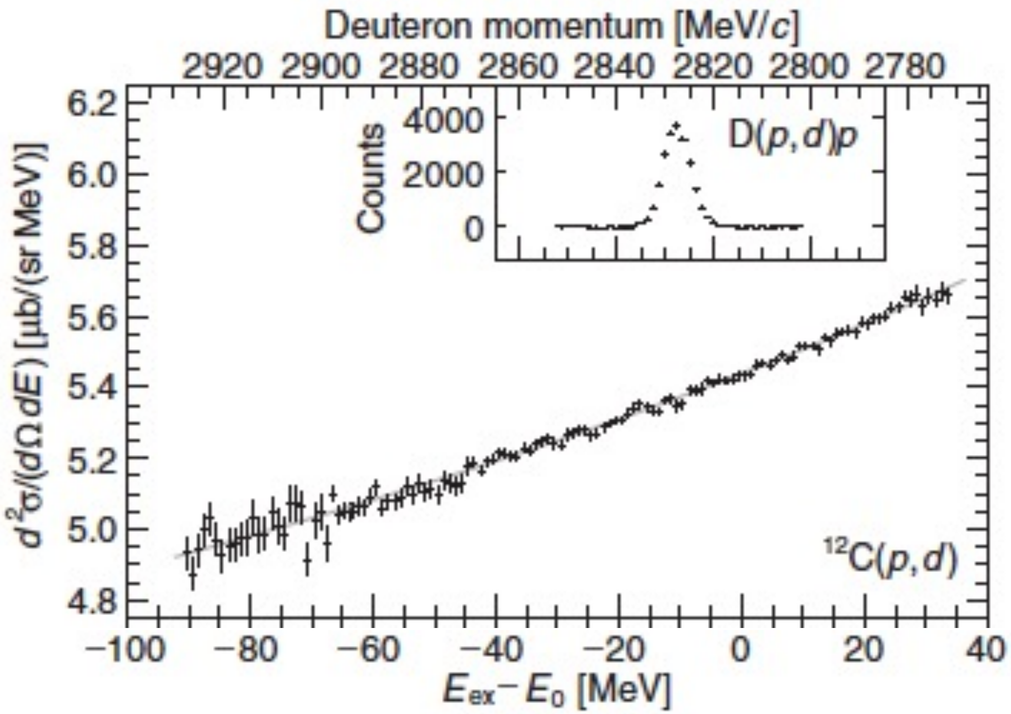

FIG. 2. (Top panel) Excitation spectrum of ^{11}C measured in the ^{12}C(p, d) reaction at a proton energy of 2.5 GeV. The abscissa is the excitation energy E_{ex} referring to the η' emission threshold $E_0 = 957.78$ MeV. The overlaid gray solid curve displays a fit of the spectrum with a third-order polynomial. The upper horizontal axis shows the deuteron momentum scale. (Inset) Deuteron

Contour on a potential parameter plane

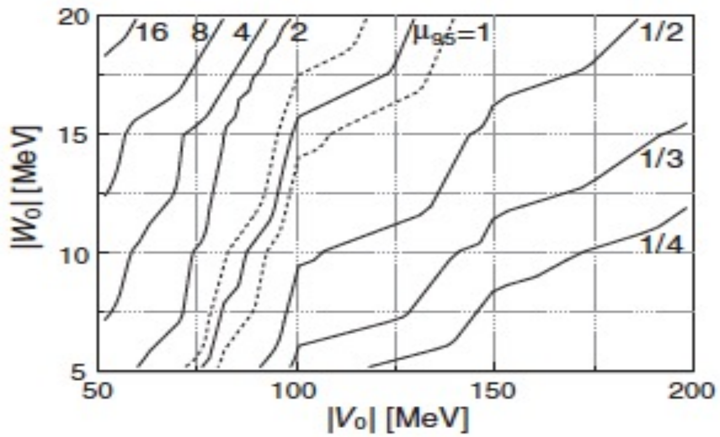

FIG. 4. A contour plot of μ_{95} (the solid curves), upper limit of the scale parameter μ at the 95% C.L., on a plane of real and imaginary potential parameters $(|V_0|, |W_0|)$. The limits have been evaluated for the potential-parameter combinations (V_0, W_0) in $\{-50, -100, -150, -200\} \times \{-5, -10, -15, -20\}$ and $\{-60, -80\} \times \{-5, -10, -15\}$ MeV and linearly interpolated in between. Dashed curves show a band of $\mu_{95} = 1$ contour indicating the systematic errors. Regions for $\mu_{95} \leq 1$ are excluded by the present analysis.

$\eta(958)$ state

- No clear peak. Upper limit is obtained.

- Data by LEPS2 (Tomida-san's talk)

- For further studies,

  - Theoretical eta(958)-N and -Nucleus interactions
  - Semi-exclusive exp. (p,dp) （WASA at FRS）

  - Self-consistent structure of eta(958)-nucleus

    => Possible Deformation (Compression) of Nucleus and Effects to the spectra.

    Meanings of the exp. upper limit may be changed.

$\eta(958)$ state

Proton kinetic energy from $\eta(958)$ decay (absorption).

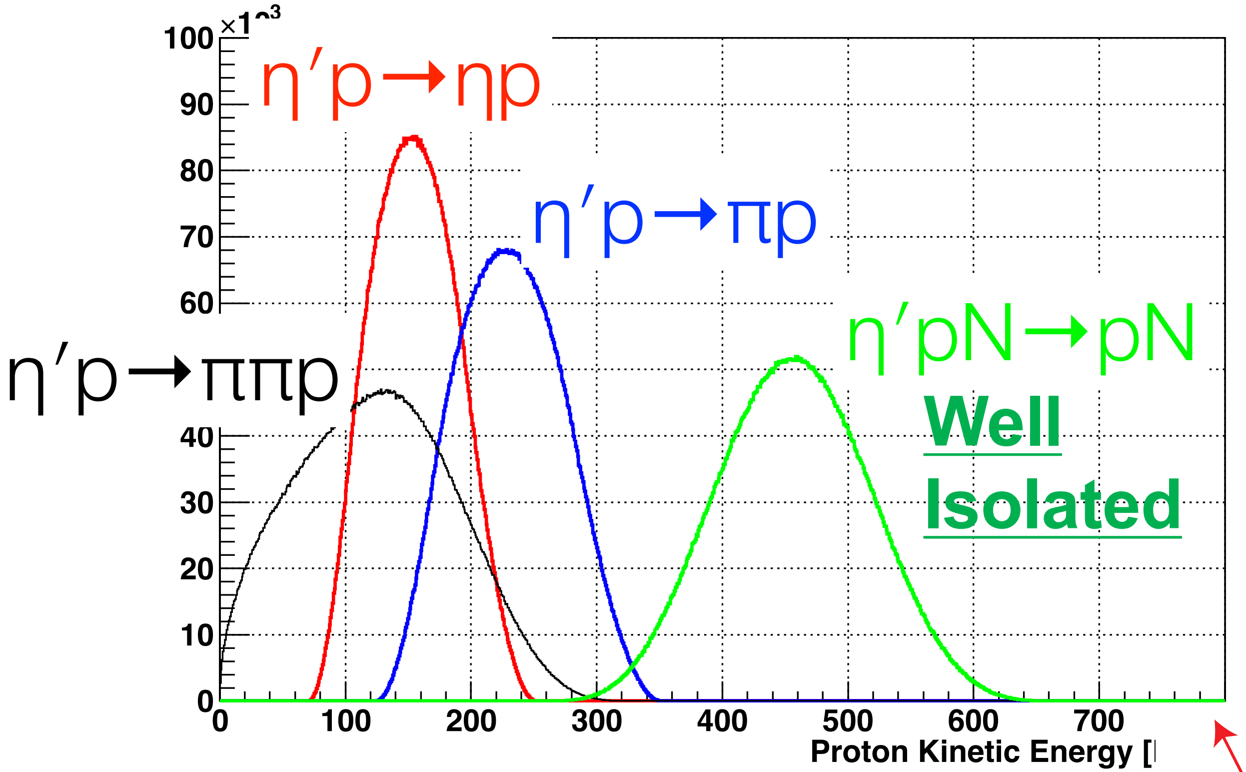

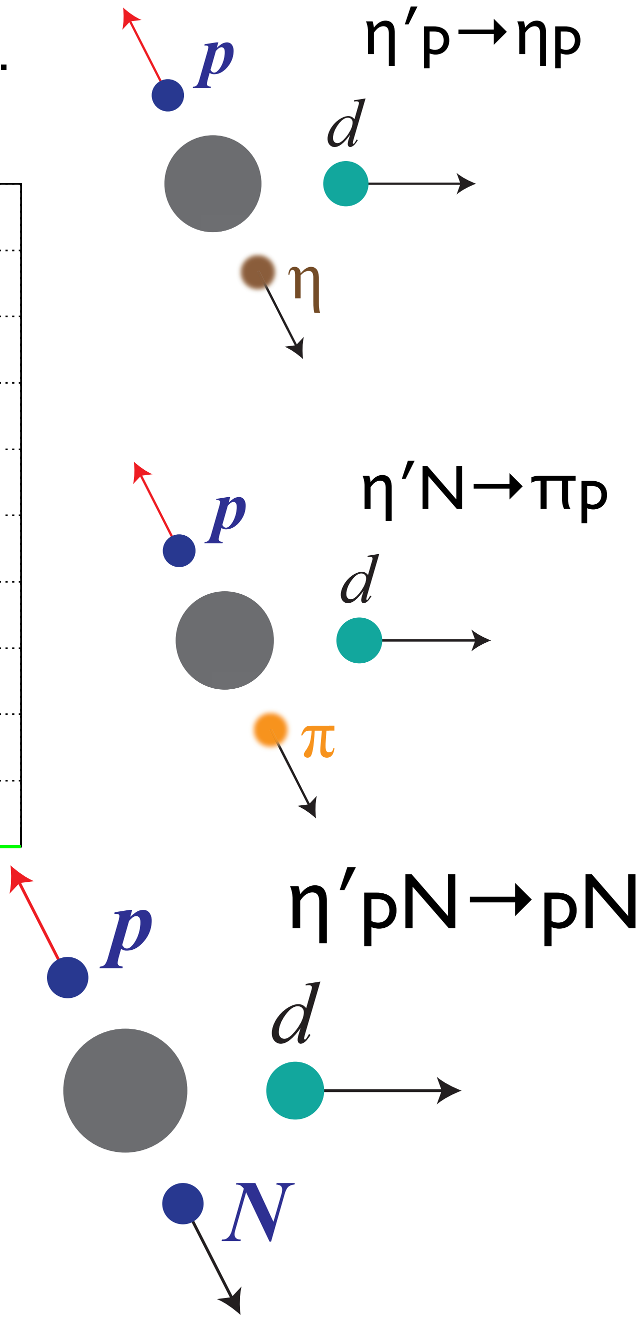

Y.K. Tanaka and Y. Higashi

$\eta(958)$ state

Simulation results: Comparison of Signal with Background

- Signal → Emitted particles from η' absorption.
- Background → Emitted particles from No-η'-processes.

To improve S/N ratio ⇒ **Focus on proton of $^{12}\mathrm{C}(p,d)p\,X$**

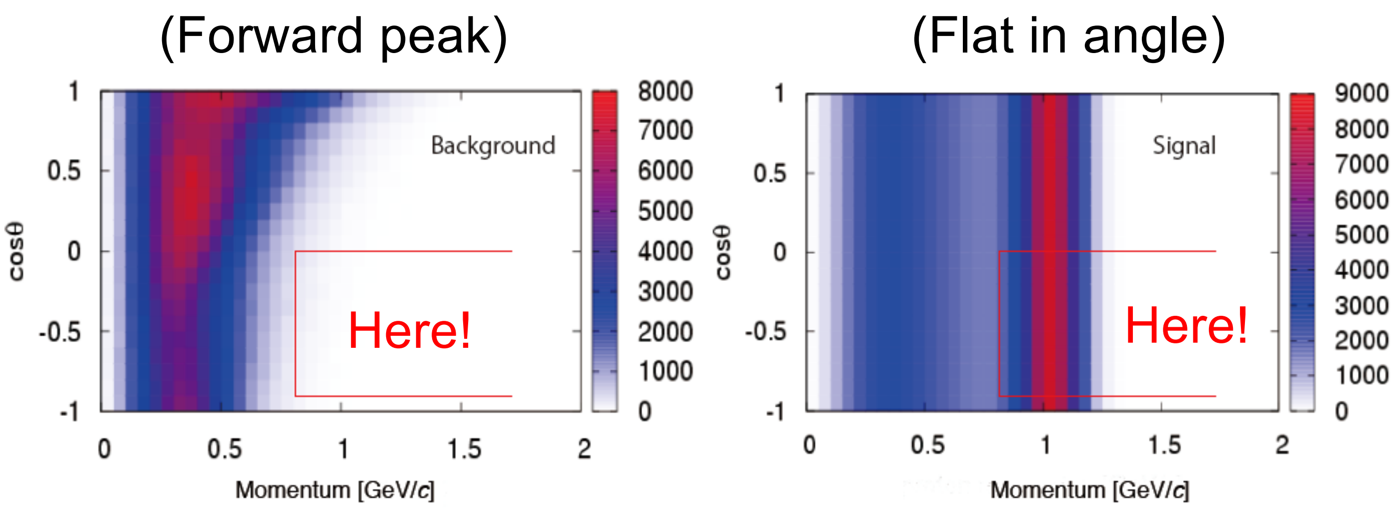

The S/N ratio could be improved by using the protons from two-nucleon absorption of η'! (proton with large momentum at backward directions seems important.) Y. Higashi (nara W.U) APS/JPS Hawaii2014

The S/N ratio is expected to be improved by the factor of ~ 100
Y. Higashi (Nara Women's U. Master Thesis (2015 Mar.))

Summary

【1】Pionic Atom at RIBF/RIKEN

Sensitivities of Observables to $\sigma_{\pi N}$

To high precision determination of $\sigma_{\pi N}$

【2】Kaonic atom in ^{3,4}He

What can be seen from data by (J-PARC E62 Collaboration)

【3】 $\eta(958)$ state in (p, dp)

Semi-exclusive data in near future

What will be seen, peak or plane ?

∗ If mass is smaller at finite density (mass shift)

→ Equivalent to Attractive pot. in Eq. of motion.

∗ Existence of Bound state and/or Attractive potential

→ NOT necessarily to be mass shift

<u>Exclusive Info. Is essential for definite answer.</u>